

Enhanced terahertz source based on external cavity difference-frequency generation using monolithic single-frequency pulsed fiber lasers

Eliot B. Petersen,^{1,2,*} Wei Shi,^{1,4} Dan T. Nguyen,¹ Zhidong Yao,¹ Jie Zong,¹
Arturo Chavez-Pirson,¹ and N. Peyghambarian^{1,3}

¹NP Photonics, Incorporated, 9030 South Rita Road, Tucson, Arizona 85747, USA

²Physics Department, University of Arizona, Tucson, Arizona 85721, USA

³College of Optical Sciences, University of Arizona, Tucson, Arizona 85721, USA

⁴wshi@npphotonics.com

*Corresponding author: epetersen@npphotonics.com

Received March 4, 2010; revised May 11, 2010; accepted May 14, 2010;

posted June 7, 2010 (Doc. ID 125012); published June 21, 2010

We demonstrate a resonant external cavity approach to enhance narrowband terahertz radiation through difference-frequency generation for the first time (to our knowledge). Two nanosecond laser pulses resonant in an optical cavity interact with a nonlinear crystal to produce a factor of 7 enhancement of terahertz power compared to a single-pass orientation. This external enhancement approach shows promise to significantly increase both terahertz power and conversion efficiency through optical pump pulse enhancement and effective recycling. © 2010 Optical Society of America

OCIS codes: 140.3070, 140.4780, 190.4223, 140.3538.

Laser development has in large part been driven by the desire to explore unused parts of the electromagnetic spectrum. The terahertz portion ($\sim 10 \mu\text{m} - 1 \text{mm}$) has recently been the focus of much of this research, specifically areas involving protein folding, imaging, and molecular fingerprinting of vibrational and rotational modes, this last application requiring spectral resolution at or below $\sim 2 \text{MHz}$ [1–3]. Terahertz generation based on optical parametric processes in a nonlinear optical (NLO) crystal, such as GaSe, ZnGeP₂ (ZGP), GaP, LiNbO₃, and DAST, using transform-limited fiber laser pulses is one of the most promising approaches, as it allows tunable single-frequency terahertz radiation with scalable power [3–7]. In terahertz generation based on single-pass configurations through NLO crystals, conversion efficiencies are typically very low. Therefore, it is very important to efficiently and coherently recycle the laser pumps to obtain high-power terahertz radiation. This must be accomplished at the same time as choosing a highly nonlinear crystal with low absorption coefficients at pump and terahertz wavelengths and selecting a laser pump with high peak/average power and narrow linewidth.

To efficiently utilize the laser pumps, we employ a ring cavity to recycle the nanosecond pulses incident onto the NLO crystal. Unlike femtosecond enhancement cavities, which employ mode-locked lasers and have achieved high enhancements, nanosecond pulses do not have a fixed phase relationship, eliminating the possibility of coherently adding them [8]. CW radiation has also been successfully enhanced, creating highly efficient second harmonic generation, whereas nanosecond pulses are not long enough to reach this equilibrium value [9]. This sparsely reported nanosecond pulse regime is ideally suited for fiber lasers and amplifiers, though, as it allows for high peak/average power scaling of the pump sources [4]. In this Letter, we demonstrate a method to produce single-frequency terahertz radiation by resonantly enhancing nanosecond pulses in an optical ring cavity then placing a

ZGP nonlinear crystal inside to perform cavity-enhanced difference-frequency generation.

The experiment consists of a 1 m ring cavity built around a ZGP crystal to perform DFG. As shown in Fig. 1, two temporally overlapped pulsed ($\sim 80 \text{ns}$, 20 kHz) fiber lasers in master oscillator power amplifier (MOPA) configuration are combined using a polarizing beam splitter and then mode matched into the cavity. The two pulsed fiber lasers are realized by directly modulating two single-frequency fiber lasers (1550 nm and 1538 nm), creating pulses with transform-limited linewidth and after DFG, correspondingly narrow linewidth at 1.5 THz. An arbitrary waveform generator was used to preshape the pulses in order to avoid pulse distortion and dynamic gain saturation in the cascaded fiber amplifiers. The pulse energy is easily scalable while maintaining transform-limited linewidth, linear polarization, and diffraction-limited beam quality, based on our newly developed large core single-mode highly Er/Yb codoped phosphate fiber in the power amplifier stage [4].

The ZGP crystal has a thickness of 4 mm with a cross section of 5 mm \times 5 mm and is double-sided antireflection coated with 10% absorption loss at $\sim 1550 \text{nm}$. This crystal was chosen because of its low terahertz absorption coefficient (0.37cm^{-1} at $200 \mu\text{m}$) and large second-order nonlinear coefficient ($d_{33} = 74 \text{pm/V}$) [10]. The cutting angle is about 7° , corresponding to the calculated internal phase-matching angle for the two pump wavelengths used. In our experiment, a type *eeo* phase-matching configuration was used, and the experimental phase-matching angle is about 9.01° . The two input beams are nearly collinear, though a slight misalignment ($\sim 1^\circ$) is needed for maximum single-pass terahertz signal owing to walk-off in the birefringent crystal. Because of this angle mismatch, the cavity resonant condition for the two wavelengths is different, and two edge filters F2 in Fig. 1 (1% loss) are needed to separate then recombine them, allowing individual cavity alignment. Two parabolic

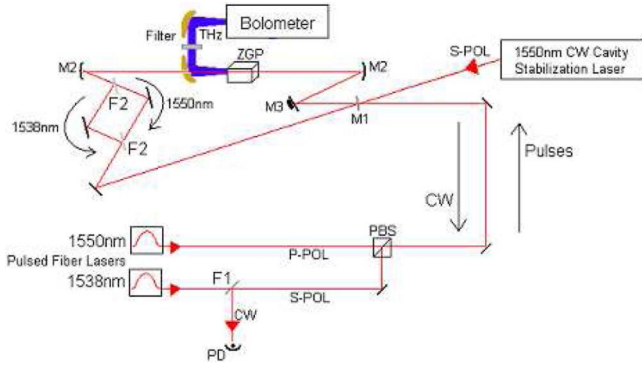


Fig. 1. (Color online) Cavity diagram including two pulsed fiber lasers and one stabilizing CW fiber laser: M1, 17% transmitting input coupler; M2, 0.25 m radius mirrors; M3, piezo-mounted mirror; F1, HR 1550 nm and HT 1538 nm filter ($\sim 5\%$ loss); F2, HT 1550 nm and HR 1538 nm filter ($\sim 1\%$ loss); PD, photodiode; PBS, polarizing beam splitter. Cavity loss of 30%.

mirrors—one with a 5 mm diameter hole to allow the pump radiation to pass through—were used to collect the generated terahertz radiation into a cooled calibrated bolometer in order to estimate the power of the generated terahertz radiation [4,5]. A black polyethylene filter was used to block any scattered pump radiation.

The cavity is stabilized by the reflected resonance of a third CW laser with wavelength of 1550 nm, as shown in Fig. 1. To avoid destabilizing fluctuations in the locking signal from the nanosecond pulses, it travels the opposite direction around the cavity to be picked off by the edge filter F1 and a photodiode, completely isolated from the other wavelengths. This signal is sent to a servo controller then to a piezo mounted on mirror M3, locking the cavity to the CW laser. The single-frequency fiber laser seeds have a fast piezo frequency control that can be used to tune them to a resonance of the cavity for a short while until the three frequencies drift apart. All three lasers are stable to <10 MHz over a 5 min period, while the FWHM of resonance for our 1 m cavity with $\sim 30\%$ losses is 14 MHz, giving ample time to make a measurement.

To achieve high peak power in the cavity, it is important to understand the dynamic pulse enhancement as a function of pulse width and cavity losses. Pulse bandwidths larger than the cavity bandwidth will not constructively interfere entirely. In addition, the pulse length is only a few times the cavity round-trip time, not long enough to approximate a CW steady state, resulting in less enhancement for shorter pulses. These are just Fourier transforms of each other and can be modeled together [11].

Following the method of [11], we sum electric field waveforms of the form $E(t, z) = E(t) \text{Exp}[i(\omega t - kz)]$ after n round trips in the cavity, where $E(t)$ is the input pulse envelope and z is the propagation direction. The cavity has electric field transmission at mirror M1 of \sqrt{T} and fractional field strength remaining after one round trip $\sqrt{1 - \alpha}$, where α is the round-trip power loss. Below in Eq. (1) is our model for pulsed electric field enhancement, where t has been replaced by $t' - Ln/c$ to model the pulse delay and confinement in the cavity. Here L is the cavity length and c the speed of light. The solid curve in Fig. 2 shows our model for pulse enhancement as a function of pulse width for the Fig. 1 ring cavity without ZGP crystal

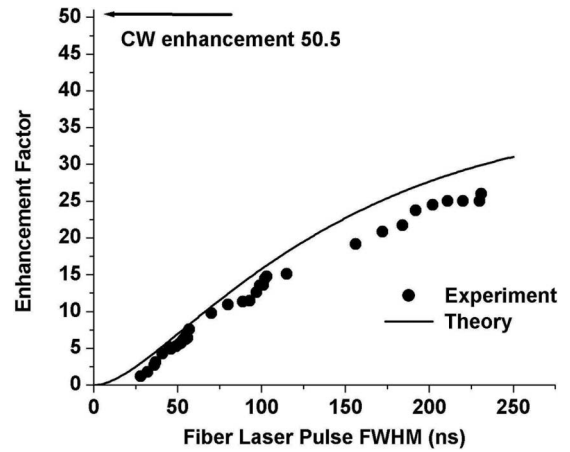


Fig. 2. Experimental (circles) and modeled (curve) pulse enhancement for 1 m cavity with 4.8% loss and 3% input transmission.

in it, assuming a Gaussian pulse. The symbols in Fig. 2 indicate the measured enhancement factor for the input laser pulses for different pulse widths. The discrepancy between experimental data and our model comes from the assumption of a Gaussian pulse envelope, which varies from our actual pulse shape shown in Fig. 3. One can see that in the nanosecond regime, the cavity enhancement factor increases with the pulse width. Our highest enhancement factor was ~ 25 when the pulse width was about 230 ns. For a CW laser, the enhancement factor is about 50.5:

$$E_{\text{cavity}} = \sqrt{T} \sum_{n=0}^{\infty} \left(\sqrt{1 - \alpha} \right)^n E(t' - Ln/c) \text{Exp}[i(\omega(t' - Ln/c) - kz)]. \quad (1)$$

To compare the fiber laser pulse enhancement for the ring cavity with and without ZGP inside, we used the exact input pulse shapes and simulated them inside the cavity. The dotted curves denote the input laser pulses, the open circles the measured cavity-enhanced pulses, and the solid curves the modeled cavity-enhanced pulses. Figure 3 shows two similar input pulse shapes and their resonant shapes for different cavity conditions. In Fig. 3(a), the modeled cavity loss and input transmission are 4.3%

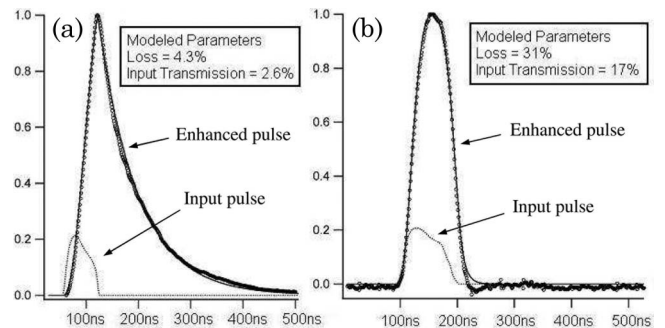


Fig. 3. Modeled (solid curve) and experimental (circles) pulse enhancement in the external ring cavity. (a) 57 ns pulse into a low-loss cavity (without ZGP); measured loss and input transmission were 4.8% and 3%, respectively. (b) 80 ns pulse to higher loss cavity (with ZGP), with 30% and 17% loss and input transmission.

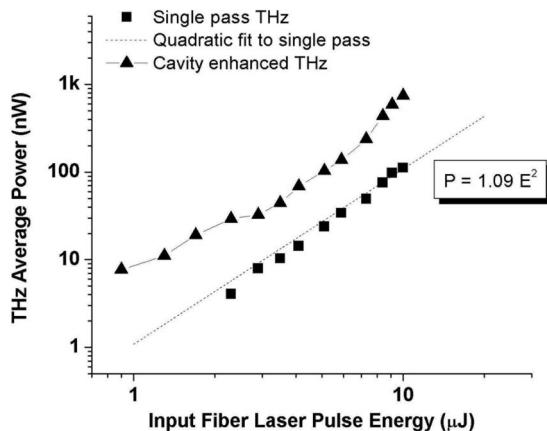


Fig. 4. Terahertz average power for input fiber laser pulse energy.

and 2.6%, respectively, while the independently measured values (from the ratio of FSR to FWHM) were 4.8% and 3.0%, the same as Fig. 2. Figure 3(b), on the other hand has much higher loss and input transmission of 31% and 17% while the measured values were 30% and 17%. In Fig. 3(a) the CW enhancement is 50.5, while in Fig. 3(b) it is 7. When the ZGP crystal is present, the cavity has higher loss with pulse enhancement looking like Fig. 3(b). One can see that the enhancement factor is 4 and depends on pulse width as seen in Fig. 2.

Figure 4 shows the average terahertz power based on DFG by using the ZGP crystal in single-pass and resonant conditions for varying input pulse energies. One can see that the single-pass data are well fit by a simple quadratic function $P = 1.09E^2$, where P expresses the terahertz average power (nW) and E the input pulse energy (μJ). This quadratic relation indicates a standard single-pass second-order nonlinear interaction [10]. The cavity-enhanced terahertz signal is obviously enhanced relative to the single pass and is not as easily fitted to a quadratic owing to variations in quality of mode matching and pulse shape differences at higher amplification levels. The highest enhancement we observed was for 10 μJ input pulses, resulting in 747 nW average terahertz power and 0.5 mW peak power, with normalized conversion efficiencies in terms of the pump peak power for single-pass and cavity-enhanced terahertz generation of $4.4 \times 10^{-3}/\text{MW}$ and $3.04 \times 10^{-2}/\text{MW}$, respectively, an improvement factor of 7. Previously, the normalized conversion efficiency was about $10^{-3}/\text{MW}$ [6]. Comparing this to the cavity enhancement of 4 as seen in Fig. 3(b), we would expect a terahertz enhancement of 4^2 . Possible reasons for not observing this factor of 16 enhancement include ensuring both channels are simultaneously resonant and a slight temporal mismatch. This result is similar to our previous work in

[12] with the addition of the third stabilizing laser. It is worth noting that overall efficiency and terahertz power can be increased dramatically for different cavity and crystal parameters. When using isotropic cubic crystals, such as GaAs and GaP, the edge filters F2 are not required, simplifying the cavity. In addition, a shorter cavity or longer pulse would allow the enhancement to build up higher, similar to that of a CW laser. If we scale the pulse energy to hundreds of microjoules to millijoules for the employed MOPA fiber lasers, the generated terahertz average power can then reach milliwatt levels and beyond.

In conclusion, we have demonstrated and modeled nanosecond pulse enhancement for two wavelengths simultaneously resonant inside an optical cavity, then we use this to show external cavity-enhanced difference-frequency terahertz generation for what we believe to be the first time. A maximum enhancement of seven times was found, compared to a single-pass orientation. We expect that this approach can be used to significantly increase the parametric terahertz power and conversion efficiency through efficient enhancement and coherent pump recycling.

This work has been supported by the U.S. Air Force Office of Scientific Research (USAFOSR) and the Joint Non-Lethal Weapons Program. The authors thank Cooney, Fernelius, Law, Schulzgen, and Jones for their technical help.

References

1. W. Shi and Y. J. Ding, *Laser Phys. Lett.* **1**, 560 (2004).
2. A. G. Markelz, A. Roitberg, and E. J. Heilweil, *Chem. Phys. Lett.* **320**, 42 (2000).
3. D. Creeden, J. C. McCarthy, P. A. Ketteridge, P. G. Schunemann, T. Southward, J. J. Komiak, and E. P. Chicklis *Opt. Express* **15**, 6478 (2007).
4. W. Shi, M. Leigh, J. Zong, Z. Yao, D. Nguyen, A. Chavez-Pirson, and N. Peyghambarian, *IEEE J. Sel. Top. Quantum Electron.* **15**, 377 (2009).
5. W. Shi and Y. J. Ding, *Appl. Phys. Lett.* **84**, 1635 (2004).
6. W. Shi, Y. J. Ding, and P. G. Schunemann, *Opt. Commun.* **233**, 183 (2004).
7. K. Kawase, T. Hatanaka, H. Takahashi, K. Nakamura, T. Taniuchi, and H. Ito, *Opt. Lett.* **25**, 1714 (2000).
8. M. Theuer, D. Molter, K. Maki, C. Otani, J. A. Lhuillier, and R. Beigang, *Appl. Phys. Lett.* **93**, 041119 (2008).
9. W. J. Kozlovsky, C. D. Nabors, and R. L. Byer, *IEEE J. Quantum Electron.* **24**, 913 (1988).
10. V. G. Dmitriev, G. G. Gurzadyan, and D. N. Nikogosyan, *Handbook of Nonlinear Crystals* (Springer, 1999).
11. R. Tanaka, T. Matsuzawa, H. Yokota, T. Suzuki, Y. Fujii, A. Mio, and M. Katsuragawa, *Opt. Express* **16**, 18667 (2008).
12. W. Shi, E. B. Petersen, J. Meair, D. T. Nguyen, J. Zong, Z. Yao, A. Chavez-Pirson, and N. Peyghambarian, *Proc. SPIE* **7631**, 76310M (2009).